Krzysztof Madej, Stefan Świdergoł, Przemysław Jakubiec

Analysis of Cracks in Welded Joints of Pipes with Eyes made of S890QL1 Steel

Abstract: The analysis presented in the article was concerned with cracks in MAG (135) robotic welded joints of pipes with eyes made of S890QL1 steel and constituting components of the latticework of self-propelled cranes. The text also presents results of tests concerning chemical composition as well as mechanical and metallographic properties of base materials and welded joints. The article contains an assessment of radial and longitudinal cracks of joints based on fractographic tests of cracks and impact-test specimens. The text also discusses the effect of welding process thermal conditions on joint properties. Test results were referred to the theory of hydrogen-induced cracking (mechanism) according to Professor E. Tasak.

Keywords: welding imperfections, welding cracks, MAG welding, S890QL1 steel

DOI: *10.17729/ebis.2015.6/2*

The research-related tests involved MAG (135) robotic welded joints of pipes with eyes constituting components of the latticework of self-propelled cranes.

The tests aimed to define reasons for the sporadic formation of cracks in joints.

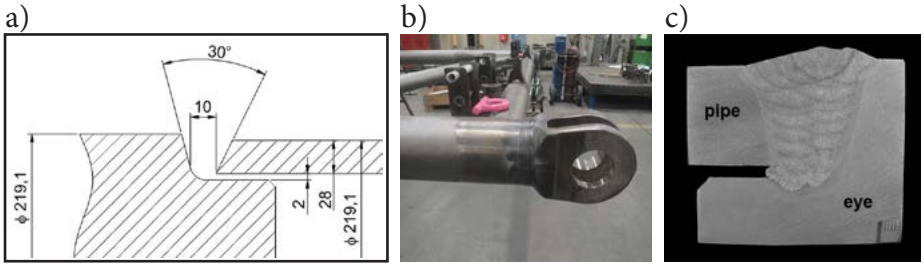

Fig. 1. Welded joint of a pipe with an eye: a – diagram of a joint, b – view of a joint, c – joint macrosection

Characteristics of joint elements:

- pipe material: S890QL1 steel – rolled element
- eye material: S890QL1 steel – forged element
- pipe dimensions: ϕ 219.1 × 28 mm

Welding process characteristics:

- electrode wire grade and diameter: G Mn4Ni2-CrMo (Thyssen Union X90); ϕ 1.2 mm
- shielding gas and its flow rate: M21; 15 l/min
- welding position: PA

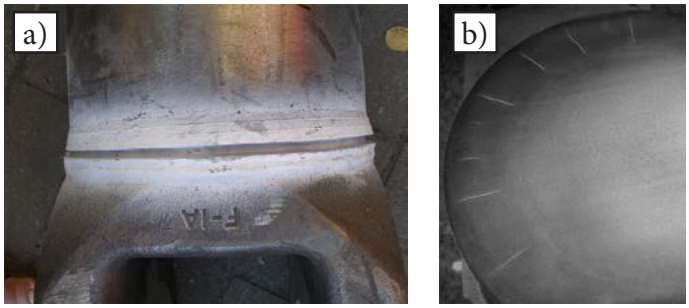

Fig. 2. Cracks in a welded joint: a – view of the joint after a penetrant test (groove indented by the manufacturer facilitated the detection of cracks), b – radial cracks on the joint cut surface along the groove

dr inż. Krzysztof Madej (PhD (DSc) Eng.), dr inż. Stefan Świdergoł (PhD (DSc) Eng.) – Instytut Spawalnictwa, Centre for Welding Training and Supervision; mgr inż. Przemysław Jakubiec (MSc Eng.) – Telemond Holding, Montel Sp. z o.o., Kostrzyn

- welding current and arc voltage: 260 A; 26 V
- arc linear energy: 16 kJ/cm
- time t_{8-5}: 11 sec.
- pre-heating temperature: 180°C
- interpass temperature: 200°C

Welded joint cracks

Penetrant tests of welded joints performed by the manufacturer revealed the presence of cracks, presented in Figure 3.

The obtainment of complete information regarding generated cracks required performing magnetic particle tests not only of radial cracks (i.e. cracks on the weld perimeter) but also of longitudinal cracks (i.e. present along the weld, in the cross-sections of the weld). The longitudinal cracks were perpendicular to the radial cracks. The cracks were present in the upper area of the weld. The cracks in transverse metallographic specimens are presented on Figure 4.

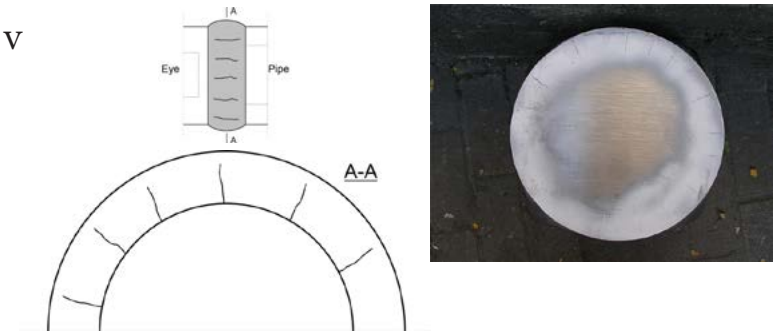

Fig. 3. Radial cracks (across the weld)

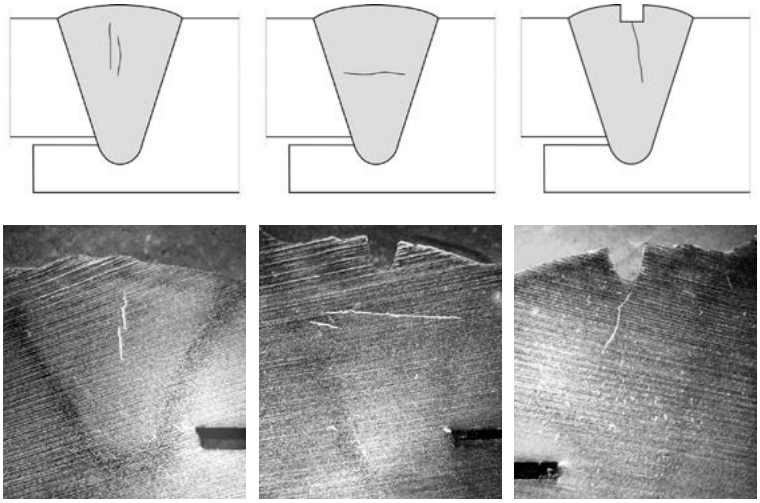

Fig. 4. Cracks along the weld – longitudinal cracks (perpendicular to radial cracks)

Material tests of the pipe, eye and weld

Table 1. Chemical composition of welded elements and of the weld (spectral analysis)

Element, %	C	Mn	Si	P	S	Cu	Cr	Ni	Mo	Al	B
Eye	0.16	0.99	0.25	0.012	0.003	0.17	1.25	2.18	0.33	0.025	0.0008
Pipe	0.16	1.50	0.30	0.020	0.003	0.11	0.59	0.15	0.36	0.042	0.0005
Weld	0.11	1.50	0.64	0.010	0.011	0.10	0.45	2.51	0.58	0.004	0.0006

Table 2. Mechanical properties of welded elements materials (round specimens parallel to the axes of elements)

Designation	R_{eH} [MPa]	R_m [MPa]	A_5 [%]	Z [%]	KV (-400°C) [J]	HV10
Pipe	890	963	19,5	70	36	300
Eye	1020	1090	18	65	110	343

The pipe material revealed a martensitic structure, whereas the eye material revealed a martensitic structure with locally present bainite and possible traces of ferrite.

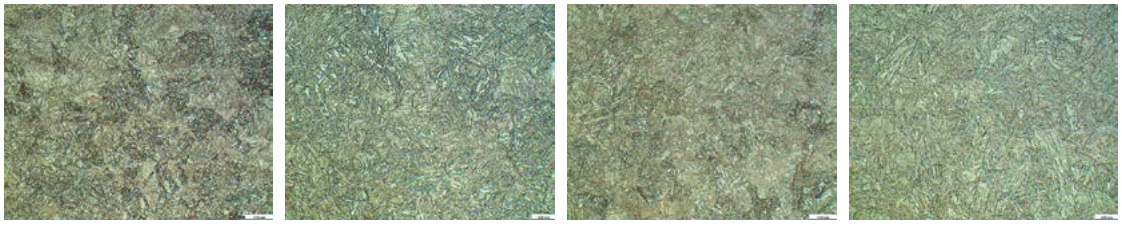

Pipe: x 200; Martensite | Pipe: x 500; Martensite | Eye: x 200 Martensite | Eye: x 500 Martensite + bainite

Fig. 5. Microstructures of the pipe and eye. Etchant: Nital

Welded joint hardness (HV10)

Table 3. Welded joint hardness results

	Eye			HAZ 1			Weld			HAZ 2			Pipe		
	1	2	3	4	5	6	7	8	9	10	11	12	13	14	15
A	345	336	348	442	409	405	306	345	342	342	387	322	297	297	304
B	330	317	327	376	383	309	309	304	333	322	309	304	299	299	304
C	312	325	317	363	394	373	348	314	330	345	317	292	304	304	304

The hardness of the joint metal in its various areas, apart from the HAZ between the eye and the weld (363-442 HV), is similar and relatively low (300-350 HV), in this respect, due to the conditions of the mutual thermal tempering of individual runs. The hardness test results

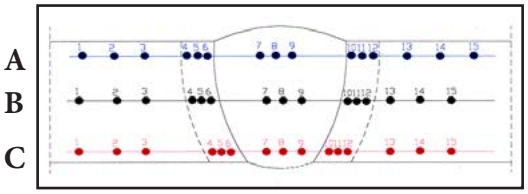

satisfy the requirements of PN-EN ISO 15614-1 (i.e. max. 450 HV for S890QL1 steel)

Radial cracks

Table 4. Hardness results (HV10) in the crack area and, for comparison, hardness of weld metal and HAZ)

Hardness in measurement point															
Weld						HAZ (pipe)			Crack						
1	2	3	4	5	6	7	8	9	10	11	12	13	14	15
317	306	322	348	322	309	390	401	390	322	294	292	333	289	309

In the direct crack area, the hardness of the metal is relatively low (289-333 HV) and comparable with the hardness of the weld (306-348 HV). Presented below is a radial crack in the cross-section along the weld – S1 and from top view – S2.

S1 x 50 top | S1 x 50 centre | S1 x 50 bottom | S2 x 50 top

Fig. 6. Radial cracks – unetched specimens

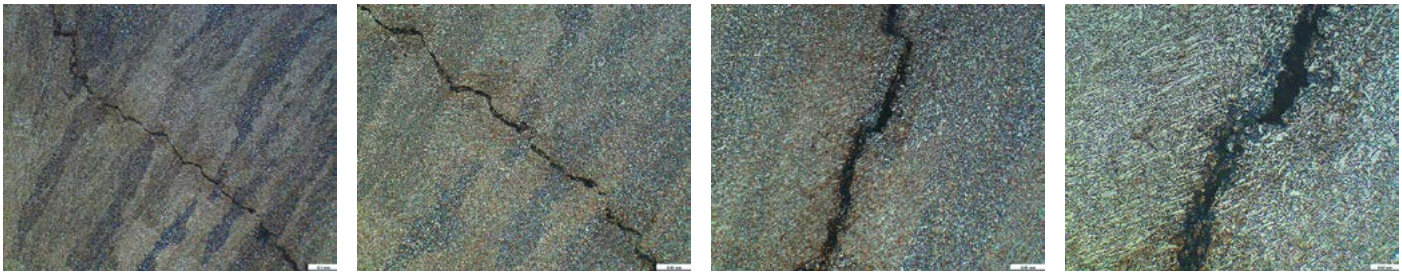

S1 weld centre x 100 | S1 weld bottom x 200 | S1 weld centre x 200 | S1 weld centre x 500

Fig. 7. Radial cracks –etched specimens (Nital)

In the crack area in the weld, there are interchangeably present bright martensite fields (dominant) and dark fields containing bainite + ferrite. The zigzag cracks are perpendicular to these fields.

Fractures of radial cracks

The figure below presents a part of the weld cut on the circumference (thickness of approximately 5 mm) with cracks and their characteristic fractures, i.e. brittle and strain-free.

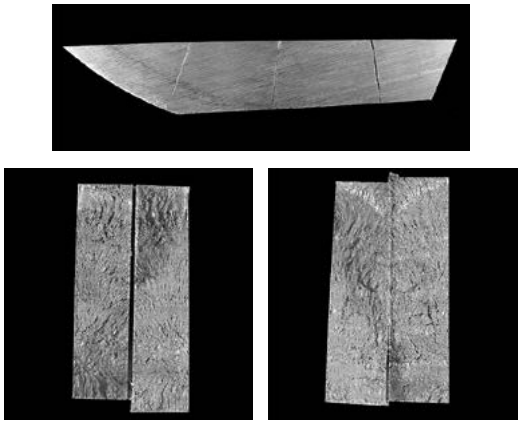

Fig. 8. Fractures of radial cracks

Fractography of radial cracks

Fractographic and microscopic tests involving the areas of radial cracks and of impact test specimen fractures were performed using a scanning electron microscope.

Figure 9 presents the results of tests involving the surfaces of the fractures of two various radial cracks. Plastic fractures dominated in both cases, yet it was also possible to observe locally present brittle fractures. On the surface of the fractures it was possible to notice the dendritic structure of successive layers of the weld.

The surfaces of the radial crack fractures revealed the presence of elongated cracks perpendicular to the radial cracks.

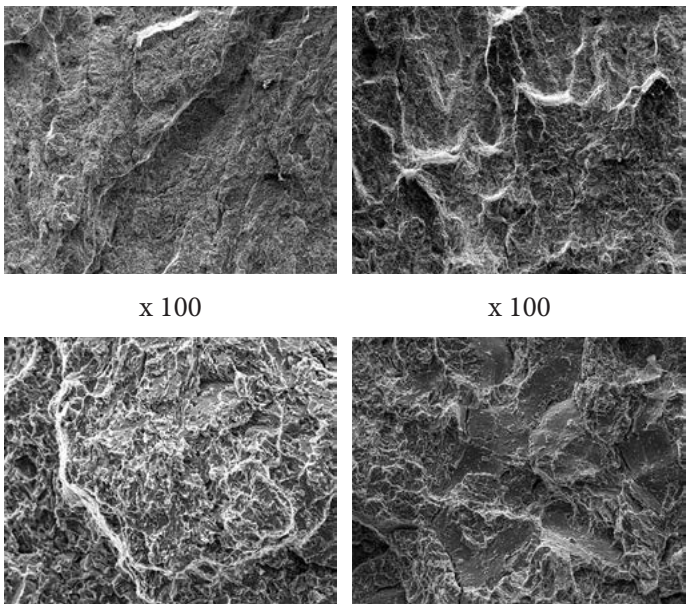

x 100 x 100

x 800 x 800

Fig. 9. Fractography of radial crack fracture

Elongated cracks

Figure 11 presents a cross-section of the elongated crack "a" from top view.

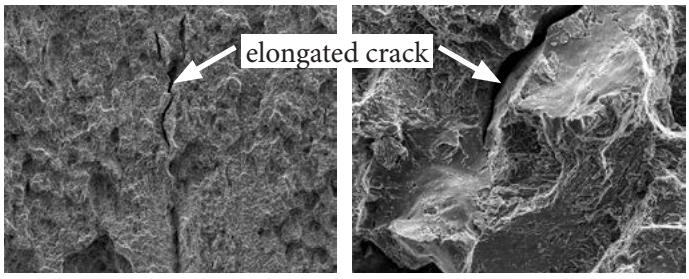

x 100 x 500

Fig. 10. Elongated cracks revealed on the surface of radial crack fractures

Impact energy (welded joint)

Table 5 presents hardness test results (impact energy) determined for the weld material and the toe angle material (between the weld and

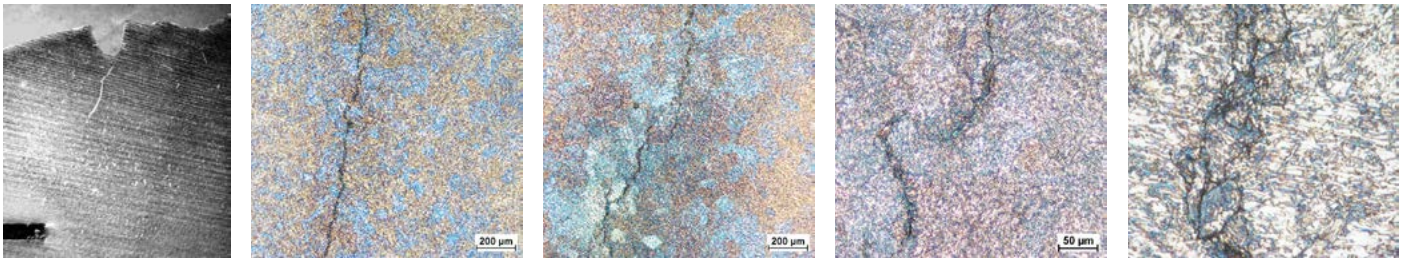

a x50 x50 x200 x1000

Fig. 11. Elongated crack

Table 5. Impact energy – welded joint

PN EN 875/PN EN 10 045-1 Requirements according to PN-EN ISO 10025-6					Notch type: Charpy V ≥ 30 J		
Specimen no.	**Testing temperature [°C]**	**Notch location***	**a_0b_0 [mm]**	**S_0 [mm²]**	**Impact energy KV [J]**	**Fracture location**	**Fracture type**
1	-40	W	8,0 x 10,0	80	28	S	brittle
2	-40	W	8,0 x 10,0	80	124	S	plastic
3	-40	W	8,0 x 10,0	80	28	S	brittle
4	-40	H	8,0 x 10,0	80	128	H	plastic
5	-40	H	8,0 x 10,0	80	138	H	plastic
6	-40	H	8,0 x 10,0	80	122	H	plastic

* W= weld, H=HAZ

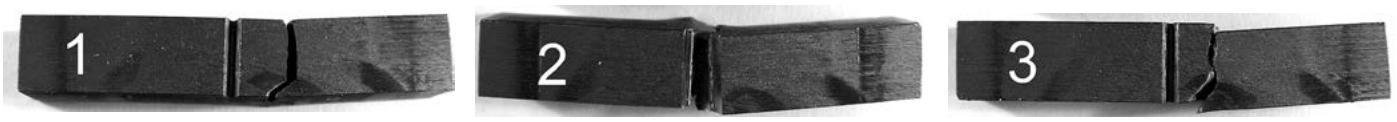

Fig. 12. Selected impact test specimens after impact tests

the pipe) (specimen sampled 2 mm under the surface). Unexpectedly, two out of the three specimens failed outside the notch (KCV=28 J), which could imply the presence of cracks in the weld outside the notch.

Impact tests (additional tests)

The unexpected results of impact strength tests (Fig. 12) were the reason for the continuation of tests using the joints of pipes.

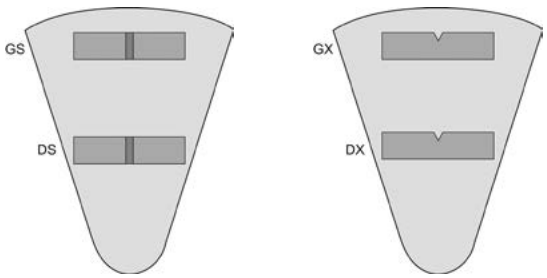

Fig. 13. Sampling locations and manner of making notches in impact test specimens

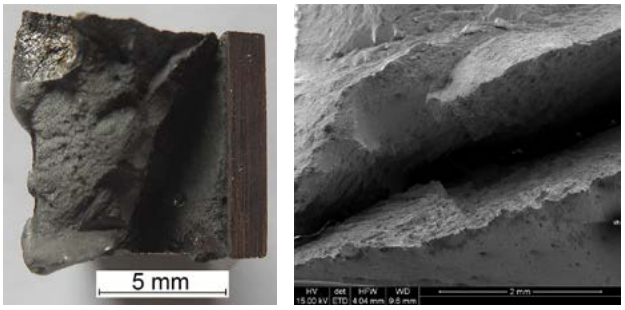

x 6 x 20

Fig. 14. Macrophotography of the fracture of specimen GS-1 with a crack

Figure 13 presents the sampling and designation of specimens.

Impact test specimen GS-1 (KCV – 114 J)

The specimen fractured in the notch. The specimen had a crack which, as a result of the fracture, opened partly. Figure 14 presents the macrophotography of specimen GS-1, whereas Figures 15 and 16 present the fractography of the fracture of this specimen. The surface of the fracture revealed the presence of brittle fracture – area "A" and plastic fracture – area "B". Figure 17 presents how the cracks in the impact test specimens penetrated their side surfaces

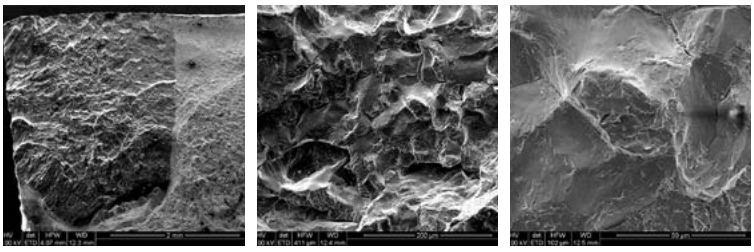

x 20 x 200 x 800

Fig. 15. Area of brittle fracture "A" in impact test specimen GS-1

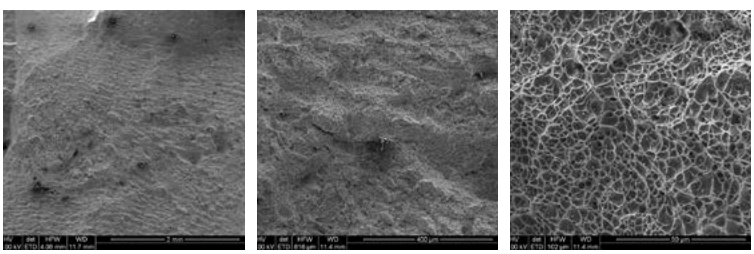

x 20 x 100 x 800

Fig. 16. Area of brittle fracture "B" in impact test specimen GS-1

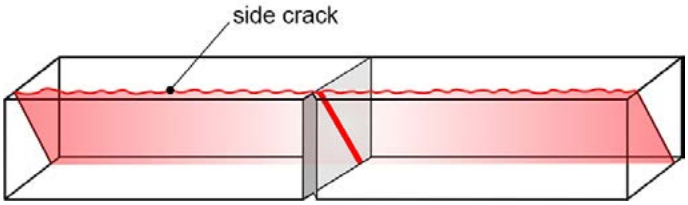

Fig. 17. Cracks on the side surface of the impact test specimen

The character of these cracks, for the sake of simplification referred to as "side cracks", was also subjected to appropriate analysis. To this end, it was necessary to make fractures of the side surface of the specimen performing macro and, also sometimes, micro observations. The edge of the fracture of specimen GS-1 revealed the presence of both brittle and plastic fracture (Fig. 18).

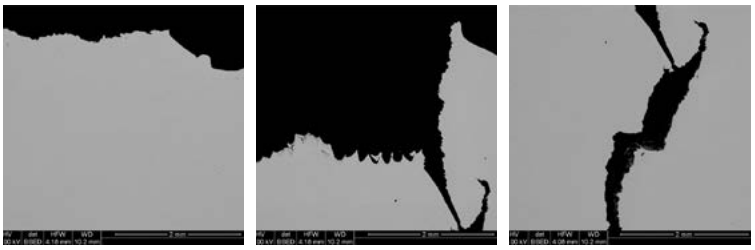

Fig. 18. Edge of the fracture of impact test specimen GS-1 with a crack

Microscopic examinations of the crack area (Fig. 19) revealed the following: a) – structure of bainite and martensite; b) – mechanical deformation of the structure; c, d) – crack along grain boundaries.

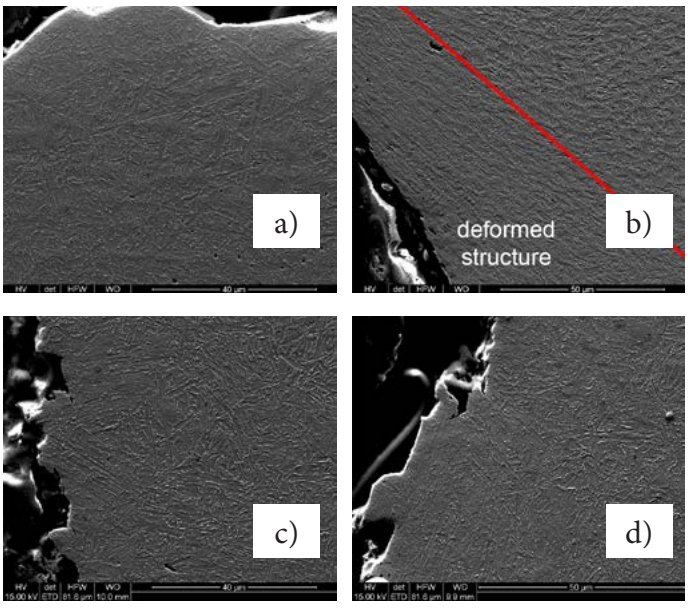

Fig. 19. Metal structure and crack edge in specimen GS-1

Impact test specimen GS-2 (KCV – 12J)

The specimen fractured outside the notch. The fracture was cleavable and the specimen was strain-free.

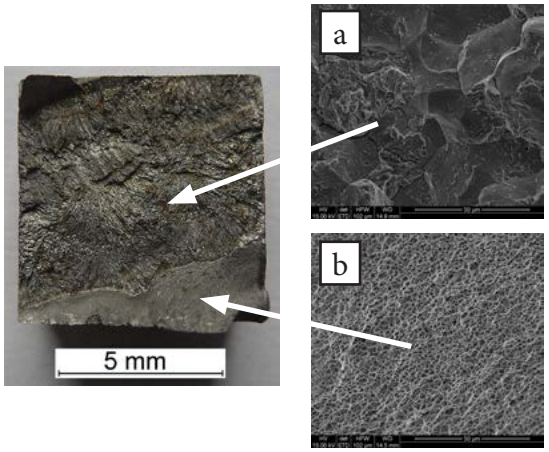

Visible bridges indicating a hot crack

Fig. 20. Fracture of specimen GS-2 containing brittle – a) and plastic – b) area

Fractographic tests revealed the presence (on the surface of the fracture) of an increased amount of brittle fracture both along grain boundaries and along boundaries of dendrites (Fig. 20 and 21) formed during the solidification of the weld. A side metallographic specimen – the shape of the upper edge is characteristic of a brittle fracture along grain boundaries (Fig. 22). Etching revealed the propagation of cracks along grain boundaries.

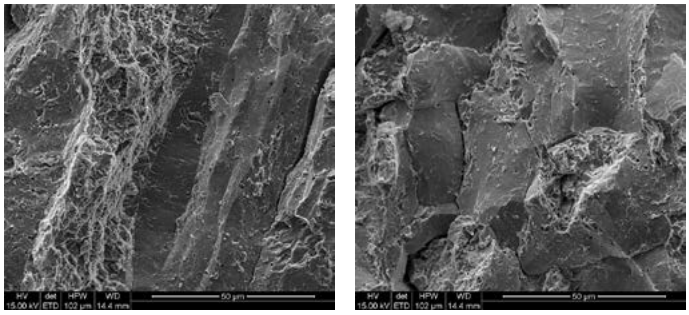

Fig. 21. Fracture along dendrites and grain boundaries with cracks between them

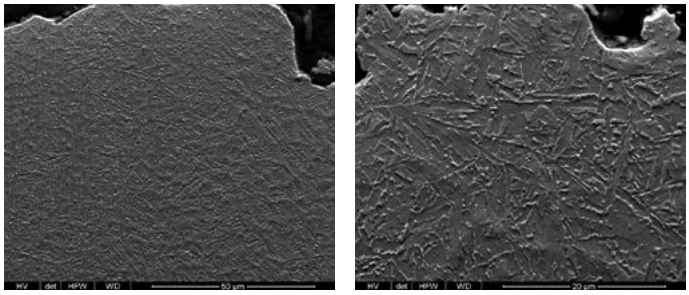

Fig. 22. Bainitic structure with visible grain boundaries

Impact test specimen DX (KCV – 54J)

The side surface of the impact test specimen revealed the intercrystalline character of the crack (Fig. 24) (metal structure – bainite).

Impact test specimen GX (KCV- 68J)

A fracture similar to that of specimen DX was also a slight crack: structure – bainite with precipitates of, probably carbides, along grain boundaries and slight amounts of tempered martensite. On the side of the metallographic specimen of specimen DX there was an intercrystalline crack.

Technological tests (additional)

Anticipating the effect of welding thermal conditions on the crack susceptibility of joints, it was necessary to make three specimens of welded joints utilising only pipes (diameter and thickness: 219 × 28 mm) made of S890QL1 steel and using similar current parameters but different welding thermal conditions resulting from the adoption of various preheating and interpass temperatures. The tests and related specimen were designated as follows:

– A: hot welding test;
– B: cold welding test;
– C: normal welding test.

- Filler metal: root layer – G4Si1;
- filling – GMn4Ni2CrMo (Thyssen Union X90).
- wire diameter – 1.2 mm;
- shielding gas – M21;
- current type and polarity – DC+.

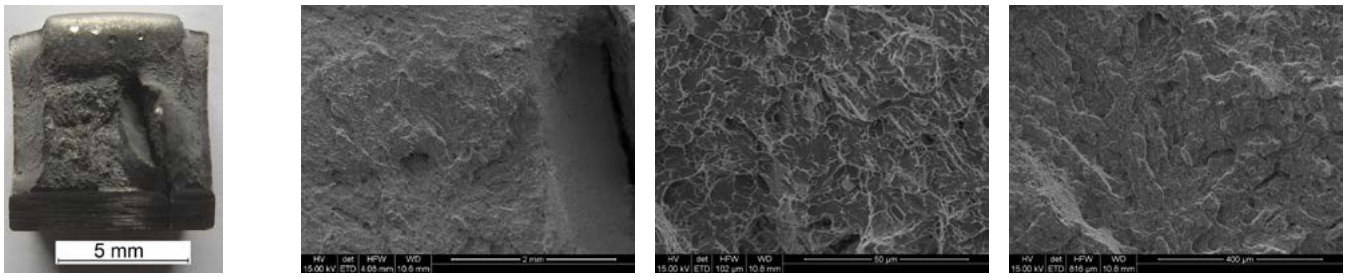

a b c d

Fig. 23. Macrophotography of the specimen fracture (a, b) with a fractographic illustration: c – primarily plastic fracture; d – at the central part – mixed fracture

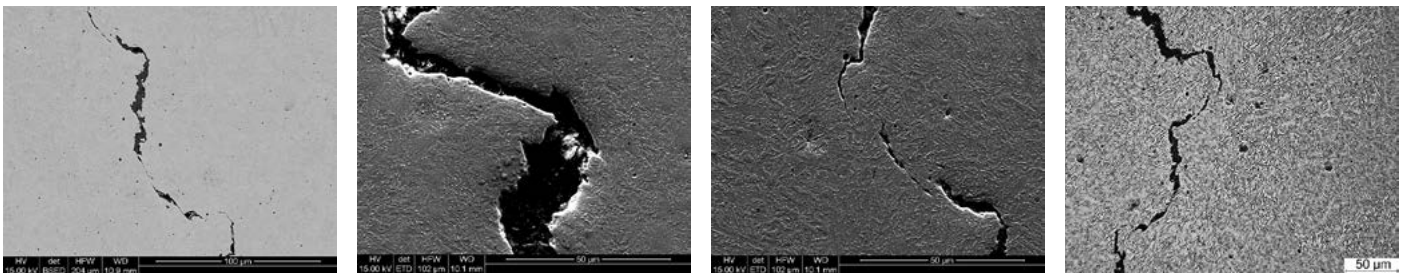

a b c d

Fig. 24. Crack on the side surface of the impact test specimen

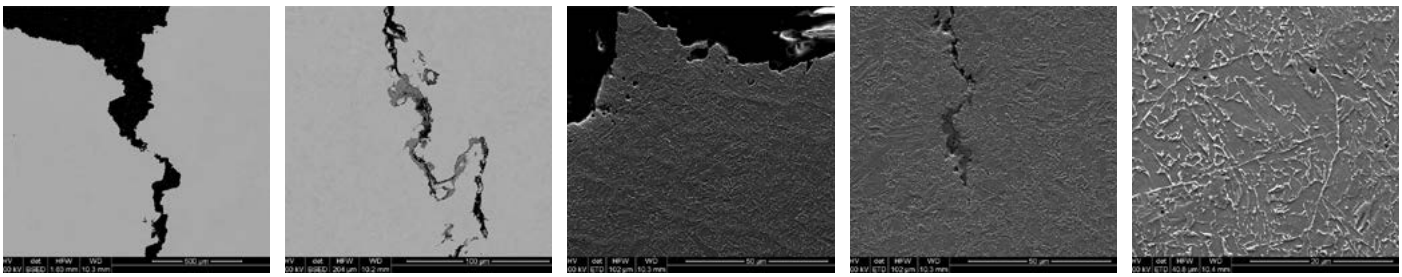

a b c d e

Fig. 25. Crack on the side metallographic specimen – a, b; upper edge of the specimen – c; a crack in the bainite area – d; bainite with precipitates of, probably carbides, along grain boundaries – e

Table 6. Parameters adopted when making joints

Welding parameters	Test A (hot welding)	Test B (cold welding)	Test C (normal welding)
1. Welding current [A]	230-260	230-260	230-260
2. Arc voltage [V]	26	26	26
3. Welding linear energy [kJ/cm]	13-18	10-11,7	10-12
4. Preheating temperature °C	200	100	150
5. Interpass temperature °C	200-300	105-130	150-250

Test A (hot welding) **Test B** (cold welding) **Test C** (normal welding)

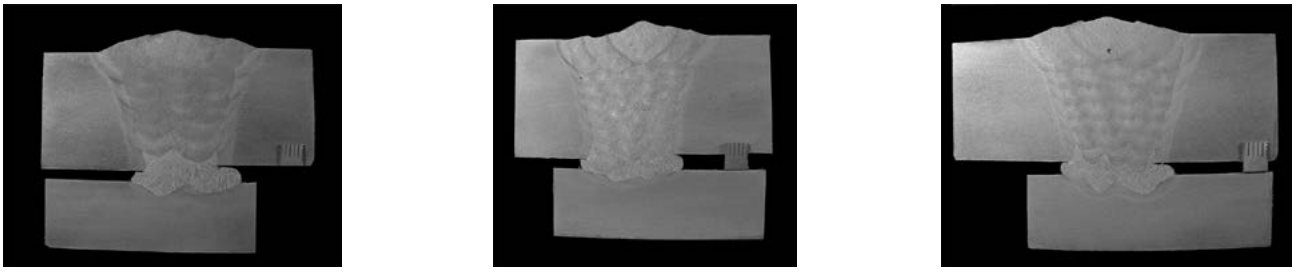

Fig. 26. Macrosections of welded joins

Selected results of tests on welded joints: impact energy, hardness and microstructure

Table 7. Impact energy (averaged results of 3 tests)

Test designation	Notch area	Testing temperature °C	Impact energy [J]
A (hot)	GS	-20	48
	GS	-40	41
	GS	-60	26 (min. 22)
	DS	-40	45
	H	-40	126
B (cold)	GS	-20	68
	GS	-40	50
	GS	-60	51
	DS	-40	52
	H	-40	148
C (medium conditions)	W	-40	54
	H	-40	120

Designations:
GS, DS – medium upper and lower part of the weld;
H – toe angle;
W – weld centre – 2 mm below the sheet surface

Analysis of cracks in welded joints

The determination of crack formation in the welded joints of pipes and eyes made of S890QL1 steel required the analysis of more important crack-formation-related issues.

Location and types of cracks in welded joints

On the basis of the cross-sections of joints and magnetic particle tests it was possible to detect radial cracks across the weld and longitudinal cracks located mainly near the weld axis (Fig. 3 and 4). In turn, analyses of the surfaces of impact test specimen fractures revealed cracks at various angles yet perpendicular to the fracture and present on the side surface of the specimen. Therefore, it could be concluded that cracks had been already present in the joint. All of the cracks observed in the impact test specimens were transverse in relation to the girth weld. The estimated number of the radial cracks was significantly greater than that of the longitudinal cracks.

Characteristics of cracks

The determination of crack types, i.e. hot, cold or post-weld cold, is of great importance due

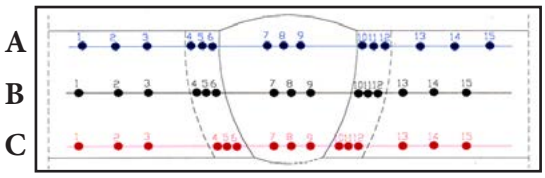

Table 8. Hardness of joints

Test A (hot welding)

	G			H			S			H			G		
	1	2	3	4	5	6	7	8	9	10	11	12	13	14	15
A, B, C	301	304	303	265	290	297	280	292	274	294	301	294	299	302	299

Test B (cold welding)

	1	2	3	4	5	6	7	8	9	10	11	12	13	14	15
A, B, C	293	293	289	294	354	346	345	367	321	327	374	319	294	285	279

Test C (medium conditions)

	1	2	3	4	5	6	7	8	9	10	11	12	13	14	15
A	299	300	302	304	314	322	299	317	316	337	306	300	295	294	282

Microstructure of joints (etchant: Nital)

Specimen A | **Specimen B**

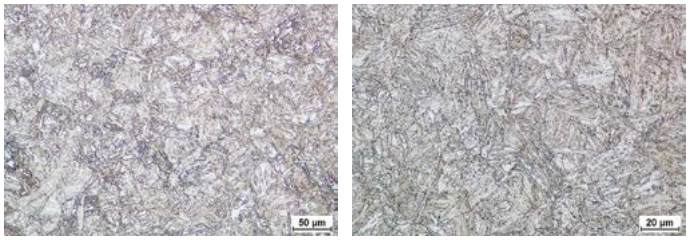

Mag. 200 × Mag. 500 × | Mag. 200 × Mag. 500 ×

Base material. S890QL1 steel. Joint thickness centre. Tempered martensite. | Base material. S890QL1 steel. Joint thickness centre. Tempered martensite.

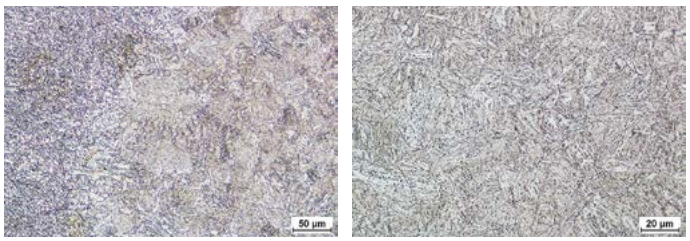

Mag. 200 × Mag. 500 × | Mag. 200 × Mag. 500 ×

Toe angle zone. Joint thickness centre. On the left – the weld. On the right - HAZ, mixture of martensite and bainite | Toe angle zone. Joint thickness centre. On the left – the weld. On the right - HAZ, martensite (little ferrite)

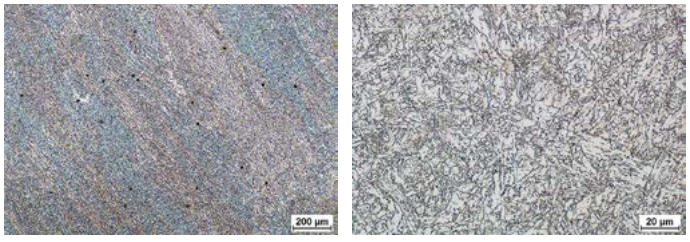

Mag. 50 × Mag. 500 × | Mag. 50 × Mag. 500 ×

Weld – another area. Joint thickness centre. mixture of martensite, bainite and ferrite | Weld – another area. Joint thickness centre. mixture of martensite, bainite and ferrite

Fig. 27. Microstructures of joints made using various preheating and interpass temperatures

to the possibility of implementing appropriate crack-preventing technological and structural procedures.

Radial cracks

The photographs of metallographic specimens present etched and unetched radial cracks (Fig. 3, 6, 7). The cracks zigzag and consist of straight segments perpendicular to interchangeably present fields of martensite and bainite. The fractures and the edges of these cracks reveal the presence of brittle and plastic fracture elements, whereas the cracks themselves are intercrystalline (transcrystalline course is difficult to assess). The material in the area of cracks (examined in the fractographic part) is mainly composed of bainite or tempered martensite of a relatively low hardness (290-300 HV). For this reason, the crack formation should be ascribed not to hardening structures but welding stresses and the negative effect of hydrogen.

Longitudinal cracks were observed on the surface of the transverse metallographic specimens of the joints and on the surface of fractographically examined radial cracks (Fig. 10, 11). The cracks observed were predominantly vertical in the weld axis and, rarely, horizontal. In several cases, the material ductility in the weld axis, verified by hardness tests, proved very low. It should be noted that hardness values of the weld centre were significantly lower than those determined in the HAZ of the joints.

Fractures of impact test specimens

In many cases, these fractures revealed the following:

- cracks skew or perpendicular to the specimen side surface; the cracks were obtuse during the impact strength tests (Fig. 14, 20, 23);
- in the fractographic tests:
  - clearly visible intercrystalline (often "stony") character (Fig. 15, 21),
  - visible gaps (cracks) between the crystallites implying hydrogen-induced hot cracks (Fig. 21) [1].

Cracks on side surfaces of impact test specimens

In one case (specimen GS2, Fig. 20), a crack was parallel to the specimen fracture surface (along the weld) and the fractography confirmed the hot character of the crack.

In the remaining cases, all of the cracks were transverse in relation to the weld. Although they were similar to radial cracks, their character was different. Visually, they were cracks with the so-called "moustache", in a straight form and with edges (often with "flourishes") revealing their intercrystalline character (Fig. 6, 7, 11, 19, 24, 25). These cracks were not subjected to fractographic tests. Near these cracks, areas of metal plastic strains were observed.

Welding stresses – metal ductility

In terms of both hot and cold cracks, stresses are primary crack-formation factors. The shrinkage of welds and structural (martensitic) transformations generate compressive and tensile stresses, which in a material of lower ductility can lead to the formation of cracks (due to the volumetric state of tensile stresses).

In order to reduce welding stresses it is necessary to ensure the following:

- joints should be made using medium-thickness runs,
- bevelling of elements being welded should be modified; in particular, it is necessary to decrease the edge gap from 10 mm to 4 mm (Fig. 1a).

Temperature of elements being welded

As regards the direct effect on cracking, the moderate heating of elements before and during welding is advantageous (hardening structures, stresses). However, overheating leads to the loss of ductility. In Germany, similar elements we welded in position PC, i.e. with reduced arc energy and possible pauses for cooling (semiautomatic welding), and the result of welding is positive. This can be adopted as one of reasons for the lack of cracks. The study-related impact

strength tests of "hot-made" and "cold-made" welds revealed only slightly better results in the second case, not satisfactory in relation to crack susceptibility reduction. As regards the strength of joints made of S890QL1 steel, the heating of elements during welding should be restricted. The adopted welding temperature-related values were the following:

– preheating temperature – 160°C,
– interpass temperature – do 250°C.

Hydrogen issue – mechanism of hydrogen-induced cracking

Until recently, hydrogen has been regarded as the reason for the generation of cold cracks during and after welding. However, hydrogen also favours hot crack generation. The mechanism of such cracking proposed by Prof. E. Tasak [1] is illustrated in Figures 28 and 29.

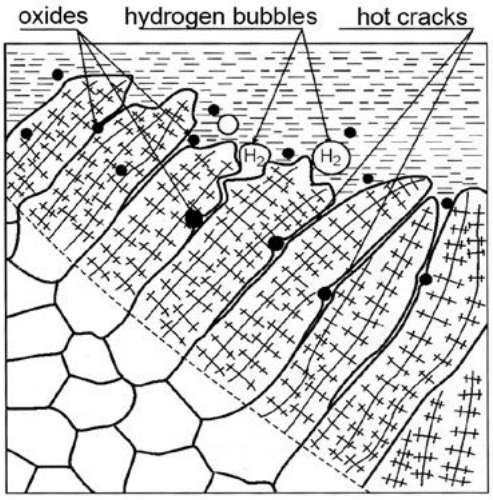

Fig. 28. Hot crack mechanism caused by excess hydrogen content

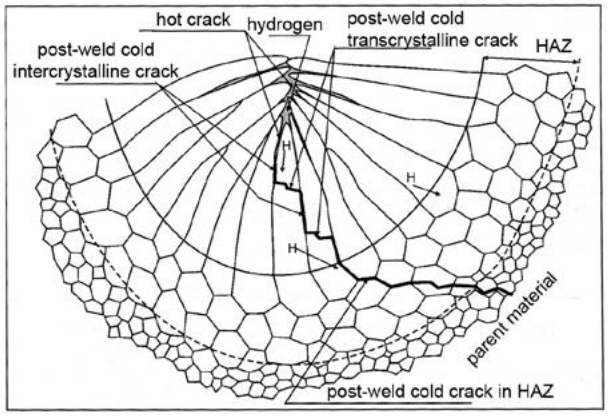

Fig. 29. Cold crack mechanism in bainitic and martensitic steels

During solidification, released hydrogen forms a gas layer between crystallites preventing their entire contact. Further diffusion of hydrogen (already in the solid-state) is accompanied by an increase in pressure and the formation of hot cracks. The cracks are thus "containers of hydrogen", which, when diffusing towards the Heat Affected Zone are responsible for the formation of (post-weld) cold cracks.

Hydrogen-induced cracks could be observed both along grain boundaries and across grains. In the HAZ, cold cracking was inter and transcrystalline in nature, whereas in the base material outside the HAZ, it was brittle transcrystalline.

Conclusions

1. The cracks present in the joint of the pipe with the eye (radial) were cold intercrystalline cracks, whereas longitudinal cracks were hot cracks. Such an assessment is justified due to the following reasons:

– shapes of cracks – with edges and tucks;
– intercrystalline character of cracks revealed by fractographic tests and courses of cracks,
– bridges visible on fractures of longitudinal cracks.

2. Hydrogen is a crack-inducing factor. In this respect, the hot crack mechanism triggered by excess hydrogen and presented by Prof. E. Tasak is reliable. In this case it is stated that longitudinal cracks are hot cracks, whereas transverse

(radial) cracks are cold cracks. For this reason, the manufacturer approached the issue of hydrogen very rigorously by introducing the following measures:

– increased cleaning of elements being welded (machining, sand-blast cleaning, chemical cleaning),
– checking the humidity of shielding gas,
– checking the humidity of air in the workshop,
– induction heating of elements,
– slowing down the post-weld cooling of elements – thermal insulation hoods.

3. Tensile welding stresses generate crack formation particularly easily in brittle hydrogen-saturated materials. In order to reduce welding stresses it is recommended that the following be considered:

– joints should be made using medium-thickness runs,
– bevelling of elements being welded should be modified; in particular, it was necessary to decrease the edge gap from 10 mm to 4 mm.

4. Since the implementation of the manufacturer-recommended process-related modifications, the formation of cracks has not been observed for 2 to 3 years.

References

[1] Tasak E., Ziewiec A.: Spawalność materiałów konstrukcyjnych. vol. 1: Spawalność stali. Kraków, 2009